



HAL
open science

Performance modeling of radiant heat recovery exchangers for rotary kilns

Antonio C. Caputo, Pacifico M. Pelagagge, Paolo Salini

► **To cite this version:**

Antonio C. Caputo, Pacifico M. Pelagagge, Paolo Salini. Performance modeling of radiant heat recovery exchangers for rotary kilns. *Applied Thermal Engineering*, 2011, 31 (14-15), pp.2578. 10.1016/j.applthermaleng.2011.04.024 . hal-00781356

HAL Id: hal-00781356

<https://hal.science/hal-00781356>

Submitted on 26 Jan 2013

HAL is a multi-disciplinary open access archive for the deposit and dissemination of scientific research documents, whether they are published or not. The documents may come from teaching and research institutions in France or abroad, or from public or private research centers.

L'archive ouverte pluridisciplinaire **HAL**, est destinée au dépôt et à la diffusion de documents scientifiques de niveau recherche, publiés ou non, émanant des établissements d'enseignement et de recherche français ou étrangers, des laboratoires publics ou privés.

Accepted Manuscript

Title: Performance modeling of radiant heat recovery exchangers for rotary kilns

Authors: Antonio C. Caputo, Pacifico M. Pelagagge, Paolo Salini

PII: S1359-4311(11)00222-5

DOI: [10.1016/j.applthermaleng.2011.04.024](https://doi.org/10.1016/j.applthermaleng.2011.04.024)

Reference: ATE 3520

To appear in: *Applied Thermal Engineering*

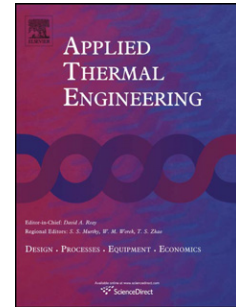
Received Date: 3 August 2010

Revised Date: 19 February 2011

Accepted Date: 12 April 2011

Please cite this article as: A.C. Caputo, P.M. Pelagagge, P. Salini. Performance modeling of radiant heat recovery exchangers for rotary kilns, *Applied Thermal Engineering* (2011), doi: 10.1016/j.applthermaleng.2011.04.024

This is a PDF file of an unedited manuscript that has been accepted for publication. As a service to our customers we are providing this early version of the manuscript. The manuscript will undergo copyediting, typesetting, and review of the resulting proof before it is published in its final form. Please note that during the production process errors may be discovered which could affect the content, and all legal disclaimers that apply to the journal pertain.



PERFORMANCE MODELING OF RADIANT HEAT RECOVERY EXCHANGERS FOR ROTARY KILNS

Antonio C. Caputo – acaputo@uniroma3.it¹

Department of Mechanical and Industrial Engineering, University of Roma Tre, Italy
Via della Vasca Navale 79, 00146 Roma, Italy

Pacifico M. Pelagagge
pacifico.pelagagge@univaq.it

Paolo Salini
paolo.salini@univaq.it

Department of Mechanical, Energy and Management Engineering, University of L'Aquila
Zona industriale di Pile, 67100 L'Aquila, Italy

Abstract. Heat loss from rotating kilns may represent a significant percentage of the total energy input especially in highly energy-intensive industrial sectors such as cement production. As an alternative to traditional energy recovery methods, the possibility of recovering radiant heat lost through the kiln surface has been proposed in the literature. This may be accomplished by surrounding the kiln with a secondary external shell acting as a heat exchanger for a transfer fluid. In this work a mathematical model for sizing and performance estimation of a heat exchanger recovering waste heat from the external surface of rotating kilns is developed. The equipment has been configured as an array of pressurized water carrying tubes arranged in a longitudinal pattern on the surface of a cylindrical outer shell coaxial with the rotary kiln. An example of model application is utilized to discuss the involved heat transfer process and its impact on equipment design. An economic model has also been developed to determine the optimal size of the equipment.

Keywords: rotary kiln, heat recovery exchanger, cement kiln, mathematical model

NOMENCLATURE

¹ Corresponding author: University of Roma Tre, Department of Mechanical and Industrial Engineering, Via della Vasca Navale, 79 - 00146 Roma, Italy (phone: +39-06-57333546; e-mail: acaputo@uniroma3.it).

a_s	Surface emissivity of kiln walls	-
a_t	Surface emissivity of HRE tubes	-
A'	Area per unit length of the cylindrical heat transfer surface	m^2/m
A_s	Surface area of the kiln shell	m^2
A_t	Surface area of the tubes bank	m^2
$c_{p,a}$	Air specific heat at constant pressure	$kJ/kg K$
c_{p,H_2O}	Water specific heat at constant pressure	$kJ/kg K$
C	Equivalent annual HRE cost	$€/year$
C_B	tubes support plates cost	$€$
C_E	Recovered heat value	$€/KWh$
C_{EHREI}	Equivalent annual HRE cost per unit length	$€/m year$
C_{HRE}	HRE capital investment	$€$
C_{HREI}	Cost per unit length of the heat exchanger	$€/m$
C_{ins}	Insulation cost	$€$
C_p	Tubes bundle cost	$€$
C_{pl}	Outer cylindrical protective shell cost	$€$
C_{uB}	Specific cost of the support plates material	$€/kg$
C_{uins}	Specific insulation cost	$€/m^3$
C_{up}	Specific cost of the adopted construction material	$€/kg$
C_{upl}	Specific cost of the adopted construction material	$€/kg$
dA_s	Differential surface area of the kiln shell	m^2
dA_t	Differential surface area of the tubes bank	m^2
d_e	Equivalent diameter of the annulus	m
d_i	Internal tubes diameter	m
d_o	External tubes diameter	m
dq_a^c	Differential convective heat flow between kiln surface and surrounding air	kW
$dq_a^{c'}$	Differential convective heat flow between air and HRE tubes	kW
$dq_{H_2O}^1$	Differential radiant heat flow between kiln shell and HRE tubes	kW
D_B	Tubes support plate average diameter	m
D_{int}	Internal diameter of tubes bundle	m
D_k	Kiln shell diameter	m
h_a	Air convective heat exchange coefficient	W/m^2K
h_{H_2O}	Water convective heat exchange coefficient	W/m^2K
H	Overall air - water heat transfer coefficient	W/m^2K
H_{fc}	Forced convective transfer coefficient between kiln and ambient air	$kcal/h m^2 °C$
H_{nc}	Free convective transfer coefficient between kiln and ambient air	$kcal/h m^2 °C$
H_{rad}	Radiant transfer coefficient between kiln and ambient air	$kcal/h m^2 °C$
H_{tot}	Overall heat transfer coefficient between kiln and ambient air	$kcal/h m^2 °C$
H_y	Yearly operating hours	$h/year$
HRE	Heat Recovery Exchanger	-
i	Annual interest rate	$%/year$
L	Reference length	m
L_{HRE}	HRE length	m
m_a	Air mass flow rate	kg/s
m_{H_2O}	Water mass flow rate	kg/s
M	Mass flow of clinker in the kiln	kg/h
MUS	Maximum unsupported tube span	m
n	Equipment operating life	$years$
N_B	Number of support plates required to hold the tubes bundle	-

N_{tt}	Tubes number	-
P_{max}	Thermal power dissipated by a bare kiln in ambient air (no HRE)	kW
P_{rec}	Recoverable thermal power	kW
Q_j	Heat dissipated in ambient air by the j-th kiln section	kW/m
Q^*_j	Heat exchanged by the j-th kiln section with air and water streams	kW/m
Q'_j	Heat uptake by the water stream from the j-th kiln section	kW/m
Q_S	Heat loss per unit mass of processed clinker	kcal/kg
R	Annual heat recovery revenues	€/year
R_{EL}	Annual revenue from recovered heat per unit length	€/m year
s_B	Tubes support plate width	m
t_B	Tubes support plate thickness	m
t_{ins}	Insulating layer thickness	mm
t_{pl}	Shell plate thickness	m
T_a	Air temperature	K
$T_{in,a}$	Air inlet temperature	K
T_{in,H_2O}	Water inlet temperature	K
T_k	Temperature of kiln shell wall	K
$T_{k,avg}$	Average temperature of kiln shell wall on the dx length	K
T_{H_2O}	Water temperature	K
T_m	Absolute mean temperature between radiating surface and environment temperature	K
$T_{out,a}$	Air outlet temperature	K
T_{out,H_2O}	Water outlet temperature	K
v_a	Air flow velocity	m/s
V	Ambient air velocity	m/s
w_p	Tube weight per unit length	kg/m
Z	Empirical constant	kcal/h °C ⁴ m ²
	<i>Greek symbols</i>	
λ	Fluid thermal conductivity	W/m K
μ	Fluid viscosity at bulk conditions	N/m ² s
μ_w	Fluid viscosity at wall conditions	N/m ² s
ρ	Fluid density	kg/m ³
ρ_M	Construction material density	kg/m ³
σ	Stefan Boltzmann constant	W/m ² K ⁴
τ	Capital recovery factor	%/year
	<i>Subscripts</i>	
s	Kiln shell	
t	HRE tubes	

1. INTRODUCTION

Portland cement is produced by means of one of the most energy intensive industrial processes (thermal energy consumption is 3100 to 7300 MJ/t, while electric energy consumption is about 147 kWh/t). As a consequence, a number of energy saving measures, like recovering sensible heat from fumes and from product cooling, have been proposed in the literature and widely applied [1]. However, a most interesting opportunity, although rarely practiced, is the recovery of thermal energy wasted from the rotary kiln external surface by heat transfer to the surrounding environment. In fact, the external surface of the kiln easily reaches temperatures of the order of 400 °C and owing to the large size of these kilns (the length may exceed 250 m, and diameter 4-6 m), heat losses from the surface are very high (about 8-15% of the total heat input). One manner to reduce this heat loss is to add a secondary insulating shell to the original kiln surface as examined by Engin and Ari [2]. However, more interesting is the adoption of external heat recovery exchangers which can be applied around the kiln and arranged in order to form a secondary shell. In this work, the recovery of waste heat from the external surface of rotating kilns is analysed by developing a detailed mathematical model for sizing and performance modelling of the required heat exchange equipment assumed as a longitudinal array of tubes arranged on the surface of a cylindrical outer shell coaxial with the rotary kiln. The model enables the solution of the coupled differential equations describing tube side and shell side convective and radiant exchange, in order to compute temperature profiles for an assigned mass flow rate of the transfer fluid, also evaluating the amount of recoverable heat. The model allows to change all the main geometrical parameters of the system in order to explore the performances of different configurations of the heat recovery apparatus. In so doing the model also acts as a design tool. In the paper, after developing the mathematical model, a discussion of the underlying heat exchange mechanism is carried out to develop insights in this heat recovery process as well as to point out some useful design criteria for the heat recovery exchanger. Finally, the economic feasibility of this heat recovery mode is discussed by developing a cost model for the heat exchanger and by analysing its economic performances as a function of the equipment length, in order to define conditions for a maximization of the net worth of the heat recovery.

2. ARCHITECTURE OF HEAT RECOVERY SYSTEM

The idea of recovering waste heat from the external surface of rotating kilns has been proposed from some time. Weinert [3] was one of the first authors to suggest such a practice also discussing a prototype application. Weinert also reported that the addition of the outer shell determined an increase of kiln shell outer temperature from 290 °C to 340 °C. This circumstance might also imply that such an energy recovery measure can even contribute to a saving in kiln fuel consumption. A

number of different embodiments of this concept, some being schematized in Figure 1, have been instead presented by Vorebechikove [4]. However, until recently, the literature discussed no specific design criteria nor any mathematical model to analyse the performance of heat recovery systems for rotary kilns adopting external heat exchangers. To fill this gap, Caputo et al. [5] presented a preliminary mathematical model of a recovery equipment configured as an array of water carrying tubes arranged in a longitudinal pattern on the surface of a cylindrical outer shell coaxial with the rotary kiln, and performed a parametric analysis to explore the performance of different equipment configurations. Subsequently, Caputo et al. [6] examined the economic feasibility of utilizing the above type of exchanger to recover waste heat from a cement kiln and feed a district heating network. Later, Söğüt et al. [7] presented a mathematical model for basically the same configuration of heat recovery exchanger. However, they discussed energy and exergy balances of the equipment within the framework of the entire plant, but did not develop a detailed model for design purposes.

Although different configurations for the kiln heat recovery exchanger (HRE) may be conceived, we assume that a tubular exchanger is utilized. In this work, the HRE is thus configured as an array of pressurized water carrying tubes arranged in a longitudinal pattern on the surface of a cylindrical outer shell coaxial with the rotary kiln (Figure 2a). This kind of arrangement allows to handle a higher flow rate of the transfer fluid, although with moderate increases of its temperature.

Conversely, architectures such as those described by Vorebechikove [4], based on plate heat exchangers or single tubes loops, allow higher transfer fluid temperatures but with a much lower flow rate. An alternative embodiment would be that of bent tubes according to a semicircular profile to match the kiln geometry as shown in Figure 2b, which more closely can resemble other literature solutions [4].

This is basically the same configuration of earlier works on this kind of equipment [5-7]. The resulting model has a general applicability and with minor changes can be easily modified to represent alternative configurations such as that pictured in Figure 2b. Accordingly, the heat transfer surfaces arrangement is schematised as that of two coaxial cylinders having infinite length. This allows to consider unitary view factors between the two surfaces. Heat transfer from tubes to the external environment is assumed to be zero. An annulus filled with ambient air exists between the two concentric heat exchange surfaces. These simplifying assumptions are valid if the tubes array circumference has a diameter close to that of the kiln shell and if the external tubes surface is insulated. Furthermore, the kiln wall temperature is assumed, at first, to be constant, but this constraint can be easily removed from the model. In this work water is assumed to be the transfer fluid flowing into the tubes array. Water was chosen owing to its low cost, flexibility of applications

and simplicity of utilization. According to the equipment configuration, multiple heat exchange mechanisms interact. Kiln external surface radiates heat towards the recovery exchanger tubes array, thus heating the transfer fluid, while it also heats the air stream surrounding the kiln surface through a convective exchange. Air, in turn, exchanges heat by convection with the heat exchanger tubes and the kiln surface. When air temperature is lower than water temperature, this convective exchange will absorb heat from the transfer fluid reducing the amount of recovered heat, while the opposite occurs when air temperature rises above the water temperature.

It is very difficult to analyze the air flow regime within the annulus, as this is the combined result of kiln shell rotation, buoyant movement of hot air along and perpendicular to the inclined kiln axis, as well as the presence of forced air streams generated from external blowers. In fact, kiln operators often install blowers along the kiln length forcing ambient air flows to impinge perpendicularly over the kiln skin in order to prevent local overheating of the kiln outer shell caused by degradation of the internal insulating layer. This is a standard practice in the cement industry, unrelated to the HRE operation, but such external streams would distribute within the annulus interacting with the existing flow field. However, additional blowers could also be installed to purposely establish a forced air stream within the annulus. From the heat transfer perspective, there is experimental evidence that free convection occurs in case of horizontal rotating cylinders in air [8], but forced convection can occur as well when the system includes air blowers. However, it is not within the scope of this model to decide whether natural or forced convection takes place, as both regimes are possible according to the specific operating conditions. In fact any air velocity could be practically achieved by installing suitable additional blowers if required by the HRE designer. Therefore, the model can work with either free or forced convection and is built to accept as an input the air flow velocity value imposed by the user instead of computing it. This means that whether free or forced convection occurs is a designer's choice. If the user is certain that only free convection occurs within the annulus he just can set a null air velocity and the model assumes a standard value for the heat transfer coefficient typical of a free convection regime. Otherwise a forced convective heat transfer coefficient is computed based on the prescribed air velocity, resorting to established correlations.

As a concluding remark, a legitimate concern may arise about whether the use of an external heat exchanger as a 'shroud' under any circumstances can interfere with the kiln operation, for instance by causing the temperature of the kiln wall to get too hot when there is no water flow. This is not a relevant problem, as any external HRE of this kind proposed in the literature is conceived with movable parts to be "opened" or removed during maintenance, during inspection of kiln walls or when there is no water flow. In our design this issue could easily be dealt with by mounting the

exchanger on a pair of rails running parallel to the kiln axis and allowing the exchanger to be moved along the kiln from the entrance section towards the colder exit section when there is no air flow. Otherwise the array of tubes could be divided into two separate arrays which are moved normal to the kiln axis to increase or reduce the annulus spacing as shown in the schemes of Figures 1b and 1c. However, a fixed heat exchanger could also be conceived. In fact, in this case the exchanger would behave similarly to a fixed shroud of insulating material which has already been suggested in the literature [2] as an energy conserving measure. When there is no water flow the fuel input to the kiln burner could be, in fact, correspondingly reduced to avoid overheating of kiln walls also contributing to a saving of primary energy.

The proposed exchanger can be applied to kilns of any length. However, the HRE will only be applied to the higher temperature section of a kiln and not to its entire length given that the temperature of kiln walls rapidly decreases passing from the inlet to the outlet section. Generally speaking, the section useful for heat recovery is in correspondence of the kiln entrance section, and it is only a few tens of meters long.

3. MATHEMATICAL MODEL OF HEAT TRANSFER

With reference to Figure 3 let x be the coordinate along kiln axis, with increasing values passing from the hot to the cold end of the kiln. Here we assume that air flows in the direction of increasing x abscissa, i.e. from the kiln inlet to outlet sections, and that water can flow in the same direction (cocurrent case) or opposite direction (countercurrent case) of air flow. The model is written for the countercurrent case.

Considering a differential kiln element of length dx , we define $dq_a^{c'}$ the convective heat flow exchanged between kiln surface and surrounding air, $dq_a^{c''}$ the convective heat flow exchanged between air and tubes, and $dq_{H_2O}^i$ the radiation transfer between kiln and tubes surface.

Energy balances for air and water across the differential element may be written respectively as

$$m_a \cdot c_{p,a} \cdot dT_a = dq_a^{c'} - dq_a^{c''} \quad (1)$$

$$-m_{H_2O} \cdot c_{p,H_2O} \cdot dT_{H_2O} = dq_a^{c''} + dq_{H_2O}^i \quad (2)$$

where m_a is the air mass flow rate, $c_{p,a}$ the air specific heat at constant pressure, T_a the air temperature, m_{H_2O} the water stream mass flow rate, c_{p,H_2O} the water specific heat at constant pressure, and T_{H_2O} the water temperature. The corresponding heat flows are

$$dq_a^{c'} = h_a \cdot dA_s \cdot (T_{k,avg} - T_a(x)) \quad (3)$$

$$dq_a^{c''} = H \cdot dA_t \cdot (T_a(x) - T_{H_2O}(x)) \quad (4)$$

being h_a the air convective heat exchange coefficient, H the overall air - water heat transfer coefficient, dA_s and dA_t the differential surface areas of the kiln shell and tubes bank respectively, and $T_{k,avg}$ is the average kiln shell wall temperature.

Convective heat transfer coefficients and H are computed according to established literature correlations, assuming forced convection.

$$h_a = 1.86 \cdot \frac{\lambda}{d_e} \cdot \left(\frac{\rho \cdot v_a \cdot d_e}{\mu} \cdot \frac{c_{p,a} \cdot \mu}{\lambda} \cdot \frac{d_e}{L} \right)^{0.33} \cdot \left(\frac{\mu}{\mu_w} \right)^{0.14} \quad \text{Re} < 2200, \text{ Sieder and Tate} \quad (5)$$

$$h_a = 0.116 \cdot \frac{\lambda}{d_e} \cdot \left(\left(\frac{\rho \cdot v_a \cdot d_e}{\mu} \right)^{2/3} - 125 \right) \cdot \left(\frac{c_{p,a} \cdot \mu}{\lambda} \right)^{0.33} \cdot \left(1 + \left(\frac{d_e}{L} \right)^{2/3} \right) \quad 2200 < \text{Re} < 10000, \text{ Hausen} \quad (6)$$

$$h_a = 0.023 \cdot \frac{\lambda}{d_e} \cdot \left(\frac{\rho \cdot v_a \cdot d_e}{\mu} \right)^{0.8} \cdot \left(\frac{c_{p,a} \cdot \mu}{\lambda} \right)^{0.33} \cdot \left(\frac{\mu}{\mu_w} \right)^{0.14} \quad \text{Re} > 10000, \text{ Sieder and Tate} \quad (7)$$

$$H = \frac{1}{\frac{1}{h_a} + \frac{d_o}{d_i} \frac{1}{h_{H_2O}}} \quad (8)$$

In the above Equations λ is the fluid thermal conductivity, ρ the fluid density, v_a the fluid velocity, μ and μ_w respectively the fluid viscosity at bulk and wall conditions, L the reference length, and d_i and d_o the inner and outer tubes diameter respectively. The equivalent diameter d_e of the annulus is computed as Kern [9]

$$d_e = \frac{D_{int}^2 - D_k^2}{D_k} \quad (9)$$

where D_{int} is the internal diameter of tubes bundle, and D_k the kiln shell diameter. Neglecting fouling resistances and tube walls conductive resistance, it may be assumed that $H \approx h_a$ as the convective coefficient is much lower for air than for water. This allows to rewrite Eq. (4) as follows

$$dq_a^{c''} = h_a \cdot dA_t \cdot (T_a(x) - T_{H2O}(x)) \quad (10)$$

The radiant heat flow transferred to water is instead

$$dq_{H2O}^i = \frac{dA_s \cdot \sigma \cdot (T_{k,avg}^4 - T_{H2O}^4(x))}{\frac{1}{a_s} + \frac{1-a_t}{a_t} \cdot \left(\frac{A_s}{A_t}\right)} \quad (11)$$

where σ is the Stefan Boltzmann constant, while a_s and a_t are the surface emissivity of kiln walls and tubes respectively. If $dA = A' dx$ is the elementary heat transfer surface area (A' being the area per unit length of the cylindrical heat transfer surface, and subscripts s and t refer to kiln shell and tubes respectively) the mass balance equations become

$$\dot{m}_a \cdot C_{p,a} \cdot \frac{dT_a}{dx} = h_a \cdot A'_s \cdot (T_{k,avg} - T_a(x)) - h_a \cdot A'_t \cdot (T_a(x) - T_{H2O}(x)) \quad (12)$$

$$-\dot{m}_{H2O} \cdot C_{p,H2O} \cdot \frac{dT_{H2O}}{dx} = h_a \cdot A'_t \cdot (T_a(x) - T_{H2O}(x)) + \frac{A'_s \cdot \sigma \cdot (T_{k,avg}^4 - T_{H2O}^4(x))}{\frac{1}{a_s} + \frac{1-a_t}{a_t} \cdot \left(\frac{A_s}{A_t}\right)} \quad (13)$$

In case cocurrent flow is assumed, Eq. (13) is written without the minus sign at left hand side. In case, instead, water flows towards the kiln outlet section the model should be changed accordingly. After some algebraic manipulations the resulting system of differential equations may be finally written as

$$\begin{cases} \frac{dT_a(x)}{dx} = -(K_1 + K_2) \cdot T_a(x) + K_2 \cdot T_{H_2O}(x) + K_1 \cdot T_{k,avg} \\ \frac{dT_{H_2O}(x)}{dx} = -K_3 \cdot T_a(x) + K_3 \cdot T_{H_2O}(x) + K_4 \cdot T_{H_2O}^4(x) - K_4 \cdot T_{k,avg}^4 \end{cases} \quad (14)$$

with the following meaning for the constants K_i .

$$\frac{h_a \cdot A_s'}{\dot{m}_a \cdot c_{p,a}} = K_1 \quad ; \quad \frac{h_a \cdot A_t'}{\dot{m}_a \cdot c_{p,a}} = K_2 \quad ; \quad \frac{h_a \cdot A_t'}{\dot{m}_{H_2O} \cdot c_{p,H_2O}} = K_3 \quad ; \quad \frac{1}{\dot{m}_{H_2O} \cdot c_{p,H_2O}} \cdot \frac{A_s' \cdot \sigma}{\frac{1}{a_s} + \frac{1-a_t}{a_t} \cdot \left(\frac{A_s'}{A_t'}\right)} = K_4$$

This system has been solved resorting to the Runge-Kutta solver of the Matlab ODE Toolbox enabling to compute the air and water temperature profiles along the kiln axial length.

In case of countercurrent flow the following boundary conditions are applied

$$T_a(x_0) = T_a(0) = T_{in,a}$$

$$T_{H_2O}(x_0) = T_{H_2O}(0) = T_{out,H_2O}$$

Where $T_{in,a}$ and T_{out,H_2O} are respectively the air inlet temperature and the water outlet temperature, while in the cocurrent case the boundary conditions become

$$T_a(x_0) = T_a(0) = T_{in,a}$$

$$T_{H_2O}(x_0) = T_{H_2O}(0) = T_{in,H_2O}$$

being T_{in,H_2O} the water inlet temperature.

The above model represents the general case when forced air convection occurs in the annulus between kiln surface and the tubes circumference, with heat transfer coefficient computed according to a user defined air flow velocity. However, if a null air velocity in the annulus is specified, the convective heat transfer coefficient assumes the free convection value (i.e. about 5 W/m² K). The same free convection value is also assumed when the forced convective heat transfer coefficient value results lower than 5 W/m² K with a non-zero air velocity specified by the user.

4. CASE STUDY

4.1 Reference plant data

The above described model has been applied to a hypothetical kiln, having a constant shell temperature, in order to show its capabilities in evaluating the performances of the examined HRE, as well as to gain some practical insights into the related heat exchange mechanism. The reference rotating kiln and HRE are characterized by the values shown in Table 1. Simulations have been carried out for HRE lengths ranging from 0 to 20 m. Overall kiln length (which is $\gg 20$ m) has not been specified. In fact, the kiln portion exceeding the heat exchanger length is not relevant for heat recovery purposes. Table 1 values are representative of actual kilns. In fact, for comparison purpose we inspected a cement kiln in Central Italy, operated by Sacci company, which was 48 m long, had a diameter of 3.35 m, a clinker throughput of 800 t/day. We measured a shell temperature passing from 389 °C to 346 °C over the first 15 m of kiln length. Temperature was roughly constant over the first 9 m of kiln length with a peak of 397 °C measured at 6 m.

4.2 Numerical results

Figures 4 and 5 compare the air and water temperature variation along the kiln axial length when a cocurrent or a countercurrent architecture is adopted, for a constant kiln walls temperature $T_k = 300$ °C and a water inlet temperature of $T_{in,H_2O} = 90$ °C. Figure 4 refers to an air velocity in the annulus $v_a = 1$ m/s while Figure 5 to $v_a = 2.5$ m/s. This fairly low velocity is plausible to arise, even without resorting to additional external blowers, when the previously mentioned factors are taken into account. If higher velocities were required then auxiliary blowers could be installed.

In the calculations it is assumed that the HRE length (L_{HRE}) is variable and assumes the values of the plots abscissa. Therefore, in Figures 4 and 5 the value of the current abscissa represents each time the overall length of the HRE, for a kiln of length $\gg 20$ m, and the plotted values represent the values assumed by the heat recovery parameters at the HRE exit when the HRE is long as the current abscissa. For abscissa values lower than the current one the plotted values show the stream parameters within the HRE. In both cases air enters the HRE from the same side of the material entering the kiln (the initial section from which the kiln abscissa starts), while water may enter the HRE from the same side (cocurrent arrangement) or from the opposite side (countercurrent arrangement). However, in order to compare the cocurrent and countercurrent arrangements, the same inlet water temperature is assumed. Table 2. shows the performances of both cases.

Both streams monotonically increase their temperature as they progress from the entrance to the exit of the HRE. However, while the behaviour in the two cases is similar, one observes that in the countercurrent solution the temperature break-even condition (i.e. when air and water temperature profiles cross and both fluids attain the same temperature) is achieved at a lower kiln abscissa. In particular, the break even abscissa is 19 m for the cocurrent arrangement while it is 15 m for the countercurrent case, when air stream velocity is 1 m/s. When air flow velocity increases to 2.5 m/s no break even occurs within the assumed maximum HRE length of 20 m. This means that in a countercurrent solution air heats up more readily and is discharged at a higher temperature.

However, for sake of heat recovery, the HRE arrangement is not relevant in practice because the contribution of convective air-water heat transfer is small respect the water heating by radiant heat transfer with kiln walls, and passing from a cocurrent to a countercurrent arrangement the water outlet temperature is only marginally affected while the discharged hot air does not constitute a heat recovery even if it subtracts heat to the kiln. Of greater impact, instead, is the air velocity. In fact when the air flow velocity increases, the overall heat uptake from the air stream increases as well owing to the higher heat transfer coefficient values, but this only produces a loss of sensible heat when the air stream is discharged at the outlet of the HRE. On the contrary, the overall heat uptake and outlet temperature of the water stream reduces due to the increasing heat flow subtracted from the air stream. In fact, while the air stream is always heated by the kiln, it only contributes to heating the water stream after the water-air break-even temperature point is reached and until air temperature remains below water temperature the air stream draws heat from both the kiln and water tubes surface. Given that increasing air velocity reduces the air temperature growth rate and increases the subtraction of heat from water to air stream, forced convection is detrimental to heat recovery. Free convection should be thus preferred for this kind of heat recovery equipment. Nevertheless free convection conditions, as already pointed out, are hardly found in practice owing to the frequent presence of auxiliary blowers for kiln cooling.

5. COMMENTS ON HEAT RECOVERY PERFORMANCES

As air and water temperature increase, both the convective and radiant power exchanged by the kiln shell decrease owing to a reduction of the driving force.

In the cocurrent case, this means that a progressive reduction of the overall heat transfer along the kiln length occurs and that the maximum thermal power absorption takes place at the HRE inlet section, while subsequent kiln sections exchange gradually lower heat flows. The overall power lost by the kiln is the sum of power lost by radiant transfer to the water tubes bank and power lost by convective transfer to the air stream, and both are of the same order of magnitude when the kiln

wall temperature is suitably high (i.e. in the order of 300-400 °C, with convective transfer becoming more relevant the lower is the kiln wall temperature). However, the thermal power transferred to the water stream, which is the useful recovered heat, is mainly constituted of the kiln radiated power and, on a much lower percentage, if any, of the convective heat transferred from the air stream to the water stream (in the HRE sections where air temperature is higher than water temperature). Therefore, owing to the interplay between the air-water convection effects, and the diminishing contribution of kiln radiation heat transfer, the thermal power dissipated by the kiln walls can not be entirely recovered by the water stream and the net recovered heat varies non linearly along the HRE length.

It should be pointed out that the amount of heat that the HRE can extract from the kiln surface depends from its design and operational parameters and in particular from the water inlet temperature and flow rate. Therefore, when high water flow rates and/or low inlet temperatures are adopted, it could happen that the HRE subtracts from the kiln a thermal power greater than the one dissipated by the bare kiln in ambient air. From a heat recovery perspective this is not acceptable as it would imply that the additional heat input should be supplied by an increased fuel consumption if the temperature regime within the kiln is to be maintained and the wall temperature is not to be lowered. Therefore, the HRE designer is constrained by the requirement that the HRE subtracts from the kiln at most the same power P_{\max} that the kiln would dissipate in the ambient air when the HRE is not applied. If, instead, the HRE subtracts less power than would be lost by a bare kiln, then the kiln walls temperature would increase and a reduced fuel consumption will follow to bring back the kiln walls temperature at usual operating values. Furthermore, while the above constraint is to be satisfied in global terms, it should be satisfied locally in any kiln section if a perturbation of the process temperature distribution is to be avoided. This imposes an even more restrictive upper bound to the amount of recoverable thermal power P_{rec} , which, in practice, is further reduced respect P_{\max} .

In fact, always referring to a cocurrent arrangement, let us consider the kiln and the HRE as ideally subdivided into a sequence of distinct sections which exchange heat (Figure 6). With reference to the generic j -th section Q_j is the thermal power that that kiln section would dissipate into the surrounding atmosphere in case no heat recovery exchanger is applied, while Q^*_j is the actual thermal power exchanged by the kiln walls with air and water streams, and Q'_j is thermal power which is recovered by the corresponding section of the heat exchanger. For a bare kiln without any heat recovery exchanger

$$P_{\max} = \sum_{j=1}^n Q_j \quad (15)$$

while the previously discussed $P_{\text{rec}} \leq P_{\max}$ constraint imposes that $Q^*_j \leq Q_j$. However, in practice, for the first section, where the heat transfer is more intense, it is strictly $Q^*_1 < Q_1$ because the required water temperature and flow rate necessary to make $Q^*_1 = Q_1$ would be unsuitable for practical use. In fact, the lower the water temperature the higher is the radiant exchange temperature difference (i.e. the exchanged power), and the higher the flow rate the lower is the water temperature increase for a given absorbed power. Furthermore, the progressive reduction of thermal power exchanged by consecutive kiln sections, owing to the gradual increase of air and water temperature which reduces the heat transfer driving force, implies that $Q^*_j > Q^*_{j+1}$. This holds with constant kiln temperature, where Q_j is also constant, but in actual applications, where kiln surface temperature gradually decreases, this effect is even more relevant. The above circumstances results in the condition

$$\sum_{j=1}^n Q^*_j < \frac{Q_1}{Q_1} \sum_{j=1}^n Q_j \quad (16)$$

As a consequence, the necessity of not increasing the fuel consumption and providing a suitable temperature level of heated water, are the main factors limiting the potential heat recovery capability of the examined equipment which is always lower than the power dissipated by a bare kiln in open air. Please note that although the trend of heat flows Q^*_j exchanged by kiln walls is monotonically decreasing, at least in a cocurrent arrangement, the trend of heat flows Q'_j uptaken by the water stream may not be monotonically decreasing owing to the contribution of air-water heat transfer. In practice, in a cocurrent arrangement, Q'_j at first may increase, because the heat uptake from the water stream to the air stream reduces more rapidly than the reduction of the radiant heat uptake from kiln walls thanks to the simultaneous air heating, and then decreases when the radiant transfer decreases more rapidly than the increase of heat uptake from air stream to water stream. This behaviour will be clear in the example of Section 6.

To assess the value of P_{\max} , heat losses to the environment from the kiln surface may be expressed, per unit mass of clinker passing through, by means of the following empirical equation valid for cement kilns [10-11]

$$Q_s = \frac{H_{tot} A_s (T_k - T_a)}{M} \quad (17)$$

where Q_s (kcal/kg_{clinker}) is the heat lost per unit mass of clinker, H_{tot} is the overall heat transfer coefficient (kcal/h m² °C), A_s is the external surface area of kiln shell (m²), T_k is the surface temperature of the kiln (°C), T_a is the absolute mean temperature of environment (°C), M is the mass flow of clinker in the kiln (kg_{clinker}/h). This equation is valid for a shell at uniform temperature. In the actual conditions this temperature assumes decreasing values from kiln burner end to the combustion gases exit end and a suitable average value should be computed. The overall heat transfer coefficient may be evaluated as the sum of radiant transfer coefficient (H_{rad}), natural convective transfer coefficient (H_{nc}) and forced convective transfer coefficient (H_{fc}) (all expressed as Kcal/h °C m²).

$$H_{tot} = H_{rad} + H_{nc} + H_{fc} \quad (18)$$

$$H_{rad} = Z \frac{(T_k / 100)^4 - (T_a / 100)^4}{T_k - T_a} \quad (19)$$

$$H_{nc} = 80,33 T_m^{-0,724} (T_k - T_a)^{0,333} \quad (20)$$

$$H_{fc} = 28,03 T_m^{-0,351} V^{0,805} D_K^{-0,195} \quad (21)$$

where constant Z , depending on the physical properties of the radiating shell, here is assumed to be $Z = 4$ kcal/h °C⁴ m² (surface not coloured, with dusty shell), T_m is the absolute mean temperature between radiating surface and environment temperature (°C), V is the mean velocity of air flow (m/s), and D_K is the outside diameter of kiln shell (m). Equations (17) to (21) are empirically derived and are here reported adopting the formulation and measurement units of the original source [10-11].

With the aim of assessing the order of magnitude of the available recovered heat respect the power dissipated by a bare kiln, Figure 7 shows the plots of lost and recovered heat as a function of HRE length and kiln wall temperature (ranging from 200 °C to 400 °C). Computations were made assuming data of Table 1, which are representative of cement plants conditions. From the figure it can be observed, for instance, that at 400 °C wall temperature, a kiln fitted with a 20 m long

exchanger would dissipate over the same length a power of about 2500 kW, but only about 1750 kW would be actually recovered, while the kiln would transfer roughly 2250 kW to both the HRE and the air stream. Nevertheless the recovered heat falls to 250 kW if the same size exchanger is utilized with a kiln having a 200 °C wall temperature.

From the above described mathematical model it can be ascertained that the heat recovery performances depend from some geometrical design parameters and some fluid related parameters which can be acted upon by the designer of the HRE. Designer selected parameters are the length of kiln equipped with the HRE, the internal diameter of the heat recovery tubes bundle (D_{int}) as well as the internal and external diameter of the water tubes. Fluid related parameters are inlet temperature and flow rate of air in the annulus between kiln surface and the bundle of heat recovery tubes, as well as the inlet (or outlet) temperature of water flowing inside tubes and its flow rate. Inlet air temperature in general may be assumed to be the atmospheric temperature unless some sort of preheating is applied. Inlet (or outlet) water temperature, instead is dictated by the requirements of the user of the recovered heat. As an example, in case hot water is used for district heating purposes it will be utilized in a primary circuit to transfer heat to a hot water distribution network for industrial or domestic heating purposes. Other relevant variables, usually not controlled by the HRE designer, are the kiln diameter (D_k) and the kiln temperature surface (T_k). Owing to the role of radiant heat transfer, in case of “cold” kilns (i.e. wall temperature lower than 250 °C), the convective power transfer is greater than the radiant transfer. In practice this implies that this kind of HRE is more suited to be applied to kiln zones where wall temperature is fairly high, while colder kiln zones could be, for instance, utilized to preheat air. When changing the water flow rate the heat transfer mechanism is not significantly affected, as the heat recovery consists mainly in radiant exchange, but water temperature is greatly affected. An increase of water flow rate obviously causes a reduction of outlet water temperature until its value might be no longer suitable for users needs.

6. ECONOMIC ANALYSIS

6.1 Estimation of HRE capital investment

The capital investment C_{HRE} (€) of the described HRE can be expressed as the sum of the tubes bundle cost (C_p , €), the tubes support plates cost (C_B , €), insulation cost (C_{ins} , €), and the outer cylindrical protective shell cost C_{pl} (€)

$$C_{HRE} = C_p + C_B + C_{ins} + C_{pl} \quad (22)$$

Referring to the constructive details of Figure 8, tubes bundle cost is

$$C_p = w_p \cdot L_{HRE} \cdot N_{tt} \cdot C_{up} \quad (23)$$

being C_{up} (€/kg) the specific cost of the adopted construction material, w_p the tube weight per unit length (kg/m), N_{tt} the tubes number and L_{HRE} (m) the length of the HRE.

The tubes support plates cost is

$$C_B = (t_B \cdot \pi \cdot D_B \cdot s_B \cdot \rho_M) N_B C_{uB} \quad (24)$$

being C_{uB} the specific cost (€/kg) of the support plates material, t_B the plate thickness (m), D_B the support plate average diameter (m) corresponding to the diameter of the circumference of the tubes bank, s_B the plate width (m) (an annular shape is assumed), and ρ_M the material density (kg/m³).

The number of support plates required to hold the tubes bundle is

$$N_B = \text{int}\left(\frac{L_{HRE}}{MUS}\right) + 1 \quad (25)$$

where MUS (m) is the maximum unsupported tube span, i.e. the spacing between two consecutive support plates. Insulation cost is

$$C_{ins} = \left[\frac{t_{ins}}{1000} \cdot \pi \cdot \left(D_{int} + \frac{d_o + t_{ins}}{1000} \right) \cdot L_{HRE} \right] C_{uins} \quad (26)$$

being C_{uins} (€/m³) the specific insulation cost, t_{ins} (mm) the insulating layer thickness, and the term in square brackets the overall insulation volume, given that insulating material is placed between the tubes bank circumference and the outer cylindrical shell. Finally, the protective shell cost C_{pl} (€) is

$$C_{pl} = \left[t_{pl} \cdot \pi \cdot \left(D_{int} + \frac{d_o + 2 \cdot t_{ins}}{1000} \right) \cdot L_{HRE} \cdot \rho_M \right] C_{upl} \quad (27)$$

being C_{upl} (€/kg) the specific cost of the adopted construction material, the term in square brackets the total shell weight, where t_{pl} (m) is the shell plate thickness.

The purchased equipment cost can be estimated adding a percentage of manufacturing cost to account for overheads, and a further percentage to account for manufacturer's mark-up.

Operating costs may include maintenance (as a percentage of capital investment) and energy expenses for circulation pumps operation. However, in this paper operating costs are neglected.

Adopting this constructive arrangement the HRE structure is fully modular, so that no economy of scale exist respect HRE length and the cost per unit length of the heat exchanger

$$C_{HREl} = \frac{C_{HRE}}{L_{HRE}} \quad (28)$$

is substantially constant.

6.2 Assessment of optimal HRE length

While the cost per unit length of the HRE is constant, the recovered heat per unit length of HRE changes when passing from a generic j -th section to the $(j+1)$ -th section along the kiln axis owing to the reduction of the heat transfer driving force (cocurrent case) as well as to the gradual reduction of the kiln wall temperature and the convective interplay between air and water streams as discussed previously. Thus, when the HRE length is increased its capital cost increases in a linear manner, but cumulative revenues from recovered heat increase at a decreasing rate. Therefore, an optimal HRE length may exist and is reached in correspondence of the section j when the equivalent annual HRE cost per unit length

$$C_{EHREl} = C_{HREl} \tau \quad (29)$$

equals the annual revenue from recovered heat per unit length

$$R_{EL} = Q_j' H_y C_E \quad (30)$$

In Equation (29) τ is the capital recovery factor

$$\tau = \frac{i(1+i)^n}{(1+i)^n - 1} \quad (31)$$

being i the annual interest rate (%/year) and n (year) the operating life, while in Equation (30) Q_j' (kW/m) is the net recovered power in the j -th HRE section of unit length, H_y the yearly operating hours (h/yr) and C_E the recovered heat value (€/KWh).

The optimal kiln length is also the one maximizing the net annual profit

$$R - C = \left(\sum_{j=1}^{L_{HRE}} Q_j' H_y C_E \right) - (\tau C_{HREl} L_{HRE}) \quad (32)$$

where R are the annual heat recovery revenues and C is the equivalent annual HRE cost.

A practical application is given in the following example, computed assuming the values of Table 1, $w_p = 4$ kg/m, $C_{up} = 3$ €/kg, $t_{ms} = 80$ mm, $C_{uins} = 500$ €/m³, $t_{pl} = 8$ mm, $C_{upl} = 3$ €/kg, $MUS = 2$ m, $s_B = 90$ mm, $t_B = 70$ mm, $C_{uB} = 7$ €/kg, $C_E = 7$ €/GJ, $H_y = 4500$ h/yr, $i = 10$ %/yr, $n = 10$ years, while manufacturing overheads are factored in as 20% of manufacturing cost, and no mark-up is accounted for. The above economic values derive from current market data for materials and industrial energy supply with natural gas in Italy. In particular the exchanger material is carbon steel given the fairly low temperature reached by water stream and exchanger tubes. Air velocity is kept here at a value of 1.5 m/s to avoid an excessive heat recovery penalization, while a variable kiln walls temperature has been assumed to increase realism. The adopted kiln temperature profile (constant temperature of 300 °C along the first 10 m of kiln length, then gradually decreasing to 200 °C in correspondence of a section 25 m from kiln inlet), although referring to a hypothetical kiln is consistent with experimental data as discussed in Section 4.1.

Figure 9 shows the temperature profiles of kiln walls, as well as water and air streams, adopting a cocurrent arrangement. No crossing of air and water temperature profiles is observed in the first 25 m of kiln length. Overall, along the 25 m of kiln length, the power transferred to air would be 422 kW, the overall power transferred to water 748 kW, while the overall power lost by kiln 1170 kW.

Figure 10 shows, instead, the exchanged heat in each section of the kiln length adopting 1 meter axial length increments. The figure portrays the overall heat lost by the kiln and the amounts exchanged with air and water streams. It appears that heat lost by the kiln when the HRE is applied is substantially lower than the power lost in open air form a bare kiln. Moreover, radiant exchange is confirmed to be the major heat transfer process. In fact, kiln walls exchange with air only about

30% of the heat exchanged with the water stream, but this percentage increases as kiln wall temperature lowers. However, the air stream subtracts heat from the water stream as well over the entire 25 m of the considered kiln length as can be seen from Figure 11. This figure depicts the total heat gain of the water stream and its constituents, i.e. the heat gained by radiant exchange with kiln walls and the heat exchanged with the air stream, which is subtracted from water stream when air temperature is lower than water temperature. Figure 11 also shows that within the first 10 meters of kiln length the rate of radiant exchange decrement is lower than the rate at which the heat subtracted by air stream reduces, so that an increasing net heat gain of the water stream is observed. The opposite happens as the rate of radiant transfer decay becomes higher than the rate of convective transfer variation.

More interesting is the economic value of the heat recovered in each kiln section. Figure 12 compares the annual revenues from recovered heat with the equivalent annual cost of each 1m – long HRE section along the kiln length. It is clear that kiln cost per unit length is constant over all sections, but the value of recovered heat changes in a non linear fashion as previously discussed. In the first 15 m each HRE section shows revenues greater than its corresponding cost so that heat recovery is economically profitable and cumulative revenues grow when the HRE length is increased. Beyond that break even point revenues from recovered heat are lower than the corresponding HRE section cost, and any further increase of HRE length determines a net economic loss eroding the cumulated profit. Figure 13 depicts cumulative revenues and cumulative HRE cost versus the HRE length, clearly showing that an optimal HRE length exist where a maximum difference between the cumulative revenues and cumulative cost occurs, corresponding to the kiln break even section. Increasing HRE length beyond the optimal one reduces the net revenues until overall cost equals overall revenues (meaning zero net worth) for a kiln length of about 35 m, as also shown in the cumulative net revenues plot of Figure 14. Further extending the HRE length beyond this point leads to a net economic loss because capital investment is not offset by cumulated heat recovery revenues. Comparing Figures 12 to 14 it is also clear that the HRE section giving the maximum net revenue (i.e. section 9) does not correspond to the optimal kiln length which, instead, correspond to the section having zero net revenue.

This kind of analysis demonstrates that this kind of HRE is only effective in the first portion of kiln length, corresponding to the high temperature zone where combustion occurs. Extending HRE length becomes readily unprofitable, and in most cases an economically optimal HRE length can be easily determined resorting to this model.

In the cited example the estimated capital investment of the optimal HRE was 250 k€, the annual revenue from energy recovery about 62.6 k€, the net present worth over a 10 years period 134 k€ and the pay back period of the HRE 4 years (discounted pay back period is 5.4 years).

6.3 Concluding remarks on heat recovery profitability

In the previous Section we showed that a HRE of the kind discussed in this paper can be economically justified. However, in this work, costs and revenues refer to the sole HRE and not to heat delivered to remote users nor include further energy conversion plants. Nevertheless, the profitability of the entire heat recovery initiative depends from site specific conditions, such as the kiln size, the value assigned to recovered energy and the kind of utilization envisaged for the recovered heat. This latter issue, in fact, may determine additional capital investments and operating cost, which can be significant especially when an off-site user is considered. However, the requested information are strictly scenario-dependent and can not be generalized easily. Therefore we focus this paper only on modelling, analysis and optimization of the heat exchanger equipment and purposely neglect issues related to the utilization of recovered heat.

In this paper reference to district heating was made as this is an option already mentioned in the literature [7]. Moreover, an unpublished study we previously carried out referred to the kiln of the Sacci company in Central Italy cited in Section 4.1, where a district heating application was sought given that the plant was located along the road connecting two villages, at a distance of 250 m and 600 m respectively. A generalized and fairly detailed parametric feasibility study of a district heating application from cement kilns was instead presented in another paper from the same authors [6] and included capital and operating costs of the entire heat distribution network. Results showed that for a recovered heat of 1.5 MW a profitable service occurs when the users are concentrated within a radius of about 100 – 200 m and the urban area is not farther than 0.5 – 1 km from the heat recovery site. If greater recoverable heat is available, and the delivery distance is moderate, then a profitable operation occurs even for a distribution radius of up to 300-400 m. On-site utilization options, instead, could include for instance low grade heat recovery for electricity generation. However, any profitability analysis of recovered energy end use is beyond the scope of this paper and should be carried out in a specific manner according to the examined scenario.

7. CONCLUSIONS

In the paper a new mathematical model has been developed for estimating the performance of radiant heat recovery exchangers applied to rotary kilns for energy saving purposes. The heat recovery equipment has been configured as an array of pressurized water carrying tubes arranged in

a longitudinal pattern on the surface of a cylindrical outer shell coaxial with the rotary kiln. The model enables the solution of the coupled differential equations describing tube side and shell side convective and radiant exchange, in order to compute temperature profiles for an assigned water mass flow rate and a given system geometry, also evaluating the amount of recoverable heat. The model may act as a design tool by allowing to change all the relevant system parameters in order to explore the performances of different configurations of the heat recovery apparatus. Utilization of the model allowed to gain useful insights about the implied heat transfer process and determine some design guidelines. In particular, cocurrent and countercurrent architectures were compared, an upper bound to the recoverable heat was defined, the relative strengths of convective and radiant heat exchange processes were assessed and the partially counterproductive role played by forced convection was put into evidence. An economic model integrated in the heat transfer model allowed to find conditions for cost effectiveness of the heat exchanger also determining the optimal exchanger length. Analysis results confirmed the technical and economical feasibility of recovering heat from kiln external surface resorting to the proposed type of heat exchanger.

ACKNOWLEDGEMENT

The authors gratefully acknowledge the contribution of Prof. Filippo De Monte of the University of L'Aquila, Italy, for the helpful comments and discussions, during the preparation of this paper.

REFERENCES

- [1] E. Worrel, C. Galitsky, Energy Efficiency Improvement Opportunities for Cement Making - An ENERGY STAR Guide for Energy Plant Managers, University of California, Berkeley, 2004.
- [2] T. Engin, V. Ari, Energy auditing and recovery for dry type cement rotary kiln systems - A case study, Energy Conversion and Management. 46 (2005) 551-562.
- [3] K.H. Weinert, Utilization of waste heat from the cement rotary kiln. Energy efficiency in the cement industry, in: Sirchis (Ed.), Elsevier Applied Sciences, London, 1990, pp. 82-87.
- [4] L.T. Vorebechikove, A device for heat recovery of rotary kilns, in: S.N. Ghosh, S.N. Yadav (Eds.), Energy Conservation and Environmental Control in Cement Industry, Vol.2, Part 1, Akademia Books International, New Delhi, India, 1996, pp. 174-181.

- [5] A.C. Caputo, M. Palumbo, P.M. Pelagagge, P. Salini, Performance modeling of radiant heat recovery exchanger in cement Kilns, Proc. CONEM 2008, 18-22 August 2008, Salvador, Bahia, Brasil.
- [6] A.C. Caputo, M. Palumbo, P.M. Pelagagge, P. Salini, District heating by radiant heat recovery from cement kilns, Proc. 12th Brazilian Congress on Thermal Engineering and Sciences ENCIT 2008, November 10-14 2008, Belo Horizonte, Brasil.
- [7] Z.Söğüt, Z. Oktay, H.Karakoç, Mathematical modeling of heat recovery from a rotary kiln, Applied Thermal Engineering, 30 (2010) 817-825.
- [8] J. T. Anderson, O.A. Saunders, Convection from an Isolated Heated Horizontal Cylinder Rotating about Its Axis, Proceedings of the Royal Society A, vol. 217 no. 1131 (May 21, 1953) 555-562.
- [9] D.Q. Kern, Process Heat Transfer, McGraw-Hill, New York, 1950, pp. 104-105.
- [10] AITEC, Ricerche, analisi e bilanci termici dei forni rotanti e verticali nell'industria del cemento. Calcoli ed applicazioni con esempi, Istituto di Ricerche dell'Industria Tedesca del Cemento (Dusseldorf), Servizio di documentazione A.I.T.E.C. n.144, 1964, (in Italian, previously in Zement-Kalk-Gips, May 1959).
- [11] AITEC, Ricerche sulla emissione esterna di calore per radiazione e convezione da parte di forni rotanti, Servizio di documentazione A.I.T.E.C. n.55, 1970 (in Italian, previously in Zement-Kalk-Gips, June 1970)

Figures captions

Figure 1. Sample configurations of heat recovery exchangers for rotating kilns (adapted from [4]).

Figure 2a - Heat exchanger with axial tubes arrangement (also shown are four tubes supporting plates).

Figure 2b - Heat exchanger with bent tubes arrangement (also shown is the main header underneath the kiln).

Figure 3- Scheme of heat exchange between kiln and water tubes (countercurrent arrangement).

Figure 4 - Comparison of cocurrent and countercurrent arrangement (air stream velocity $v_a = 1$ m/s).

Figure 5 - Comparison of cocurrent and countercurrent arrangement (air stream velocity $v_a = 2.5$ m/s).

Figure 6 - Rotary kiln schematization.

Figure 7. Lost and recovered heat vs HRE length in comparison with power dissipated by a bare kiln.

Figure 8 - Rotary kiln HRE constructive details.

Figure 9. Temperature profiles.

Figure 10. Trend of heat exchanged by kiln. Legend: Kiln loss (model) = overall heat lost by kiln walls when the HRE is installed; Kiln loss (AITEC) = overall heat dissipated by kiln walls in open air without HRE; d_{qi} = radiant heat transferred by kiln walls to water stream; d_{qac1} = heat exchanged by convective transfer between kiln wall and air stream.

Figure 11. Trend of heat exchanged by water. Legend: Net gain H₂O = overall heat acquired by water stream; d_{qi} = radiant heat transferred by kiln walls to water stream; d_{qac2} = heat exchanged by convective transfer between water and air stream.

Figure 12 Annual revenues compared with equivalent annual cost on a section by section basis.

Figure 13. Cumulative annual revenues and capital investment vs HRE length.

Figure 14. Cumulative net annual revenues vs HRE length.

Table 1. Characteristics of sample rotating kiln.

D_k	4.0 m	$T_{in,a}$	15 °C
D_{int}	4.5 m	d_o	20 mm
T_k	300 °C	d_i	16 mm
$T_{in,H2O}$	90 °C	L_{HRE}	20 m
m_{H2O}	10 kg/s	$Tubes\ pitch$	$d_o + 20\ mm$

Table 2. Heat recovery performances (20 m long HRE).

	Cocurrent	Counter current	Cocurrent	Counter current
v_a (m/s)	1.0	1.0	2.5	2.5
$T_{a,out}$ (°C)	115.8	114.9	62.9	62.8
$T_{out,H2O}$ (°C)	110.9	110.9	109.5	109.5
Air and water temperature profile crossing abscissa (m)	19	15	No intersection	No intersection
Overall power transferred to air (kW)	353	350	454	453
Overall power transferred to water (kW)	879	879	822	822
Overall power lost by kiln (kW)	1233	1229	1276	1274

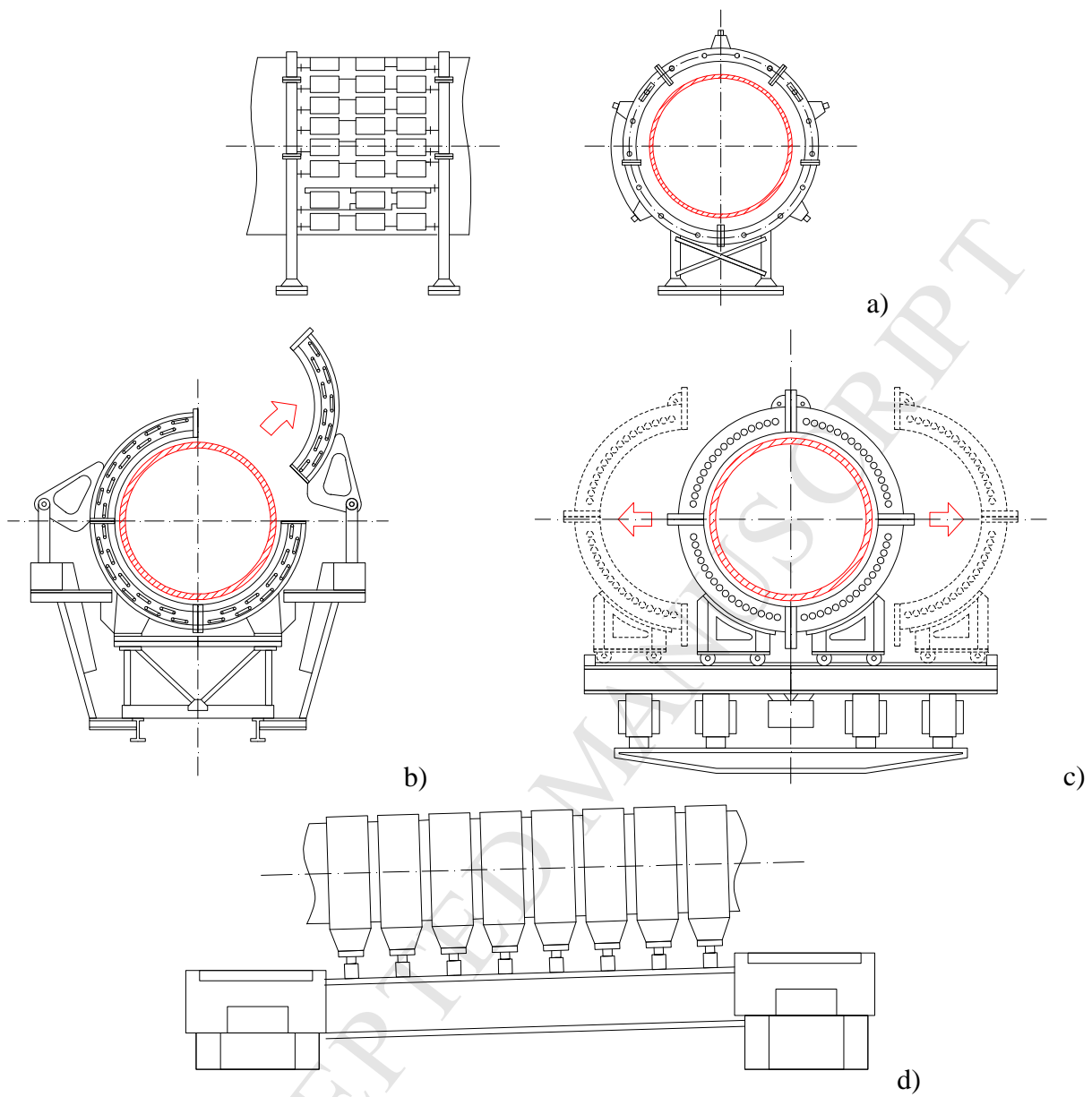


Figure 1. Sample configurations of hear recovery exchangers for rotating kilns (adapted from [4]).



Figure 2a. Heat exchanger with axial tubes arrangement (also shown are four tubes supporting plates).



Figure 2b. Heat exchanger with bent tubes arrangement (also shown is the main header underneath the kiln).

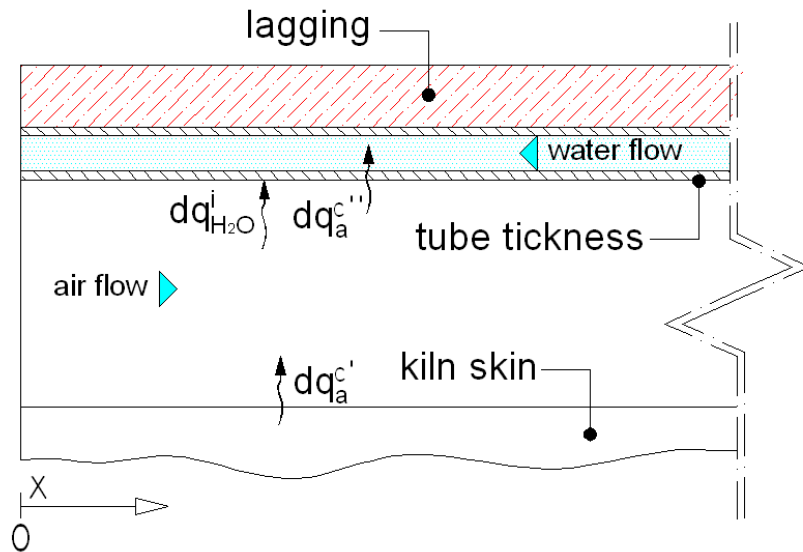


Figure 3. Scheme of heat exchange between kiln and water tubes (countercurrent arrangement).

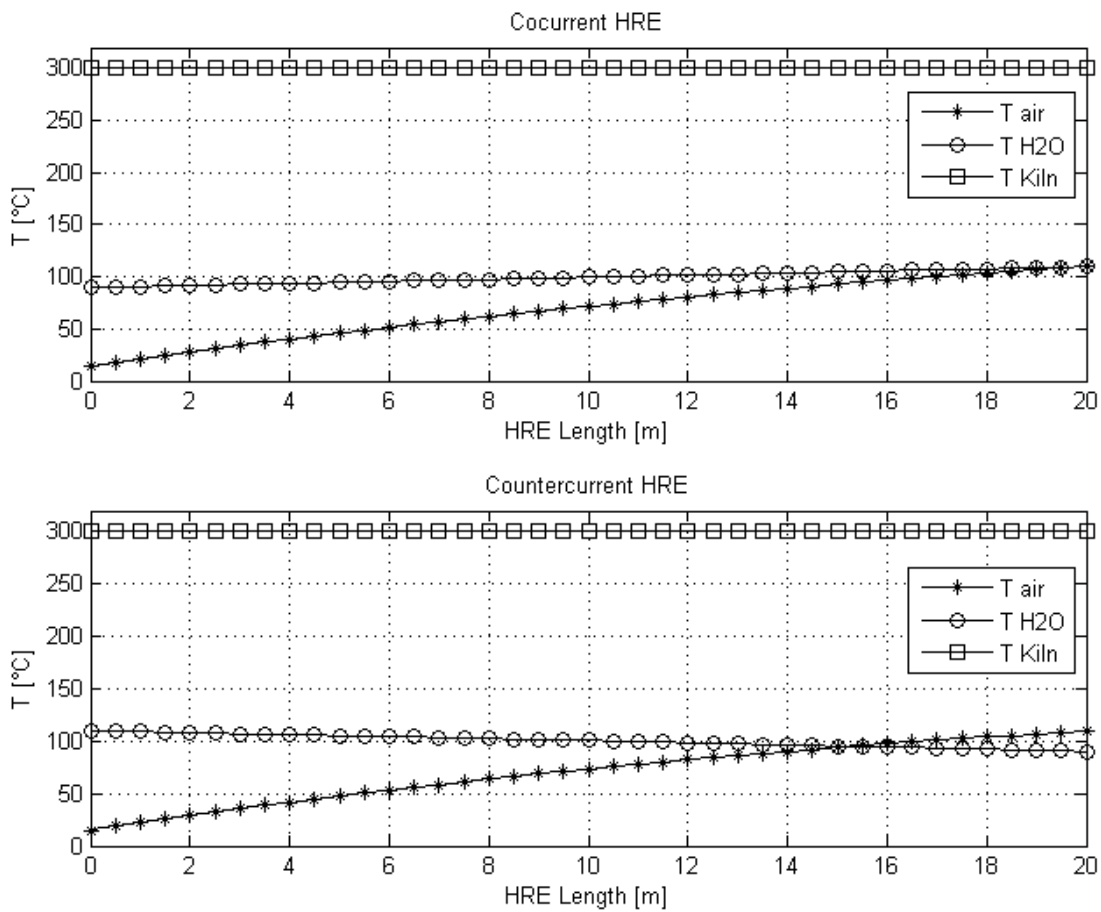


Figure 4. Comparison of cocurrent and countercurrent arrangement (air stream velocity $v_a = 1$ m/s).

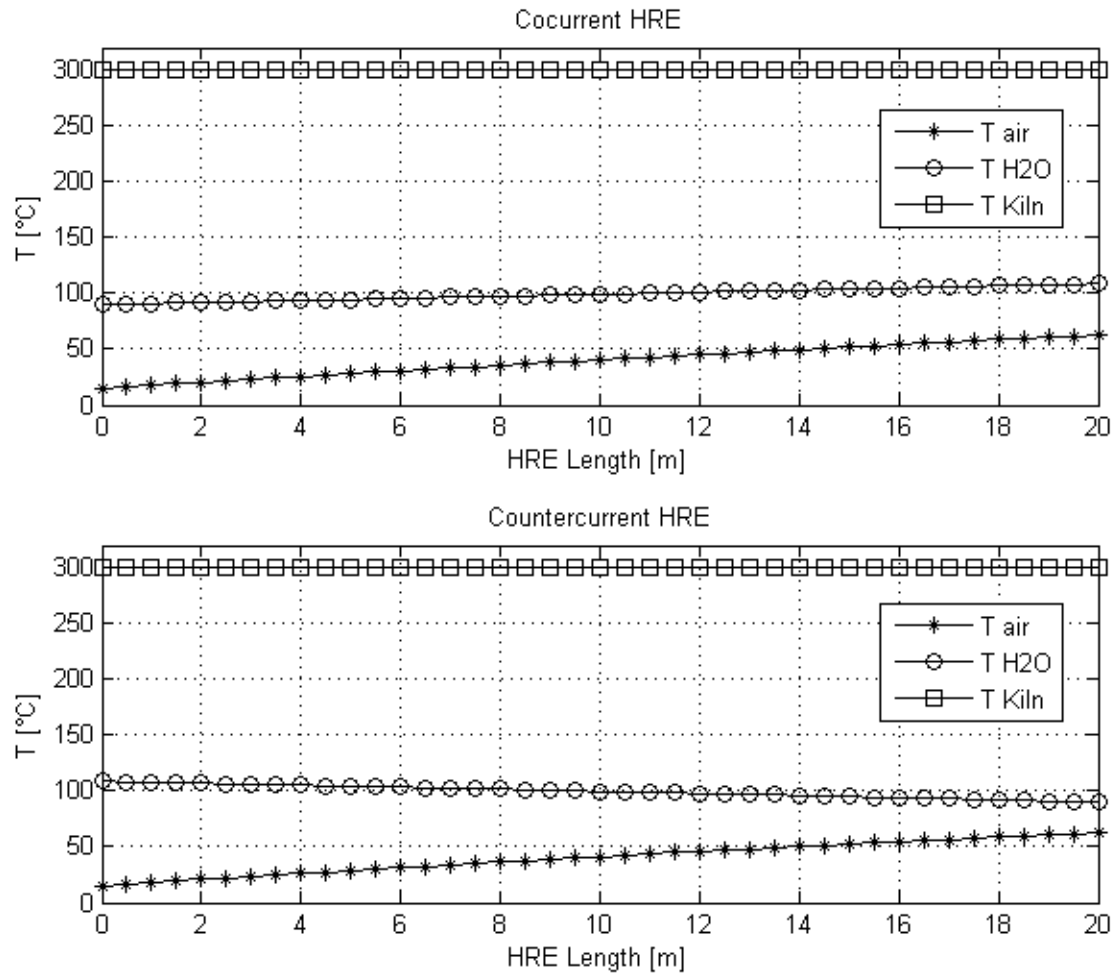


Figure 5. Comparison of cocurrent and countercurrent arrangement (air stream velocity $v_a = 2.5$ m/s).

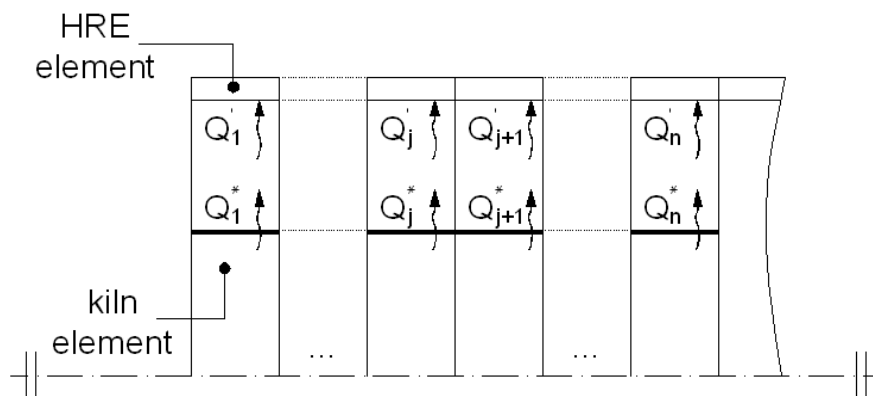


Figure 6. Rotary kiln schematization.

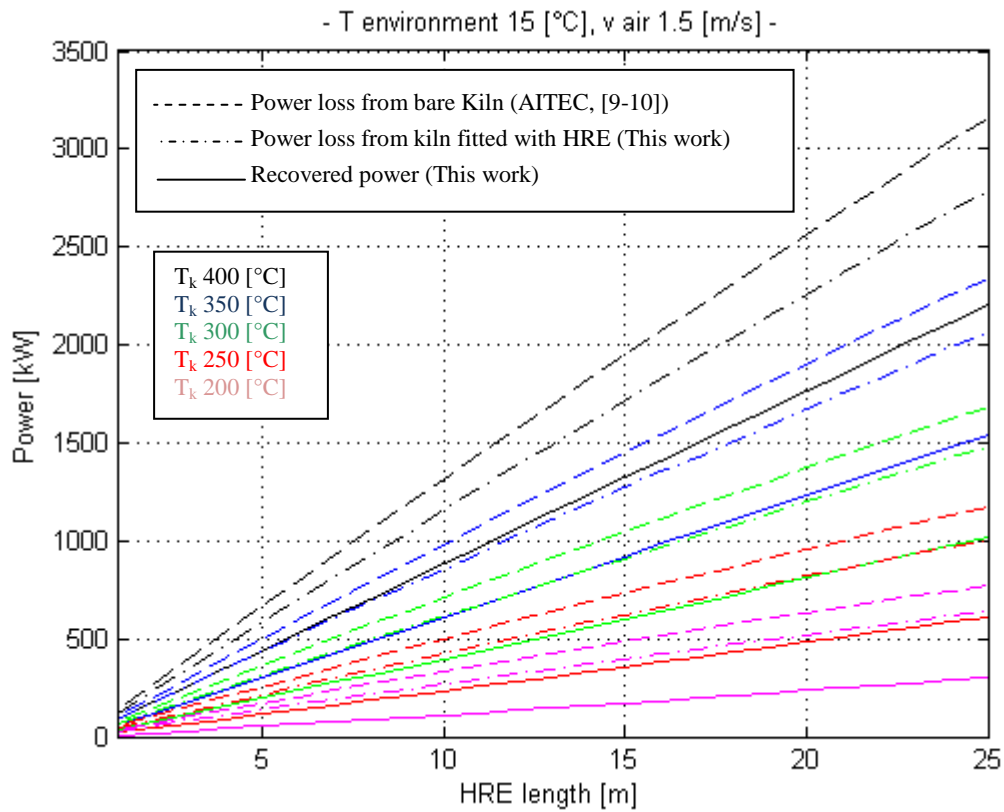


Figure 7. Lost and recovered heat vs HRE length in comparison with power dissipated by a bare kiln.

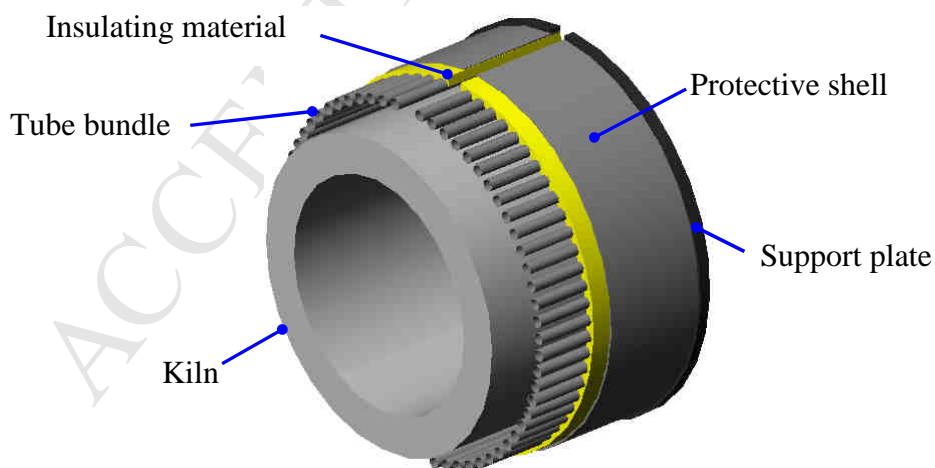


Figure 8. Rotary kiln HRE constructive details.

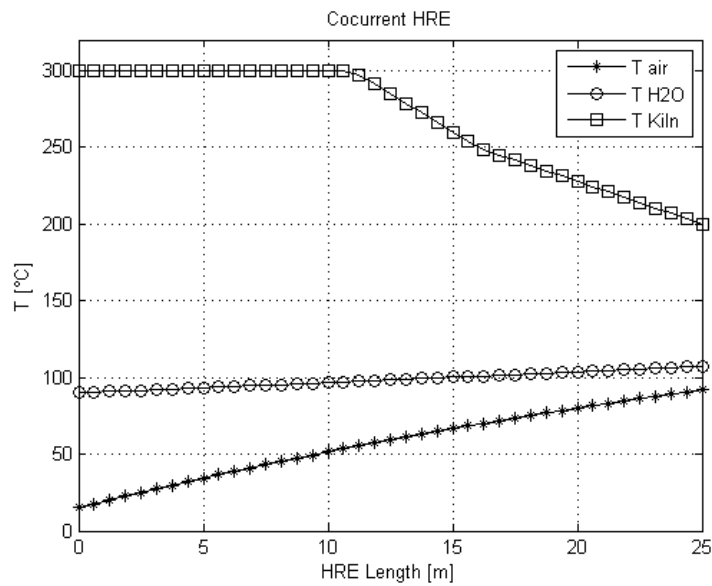


Figure 9. Temperature profiles.

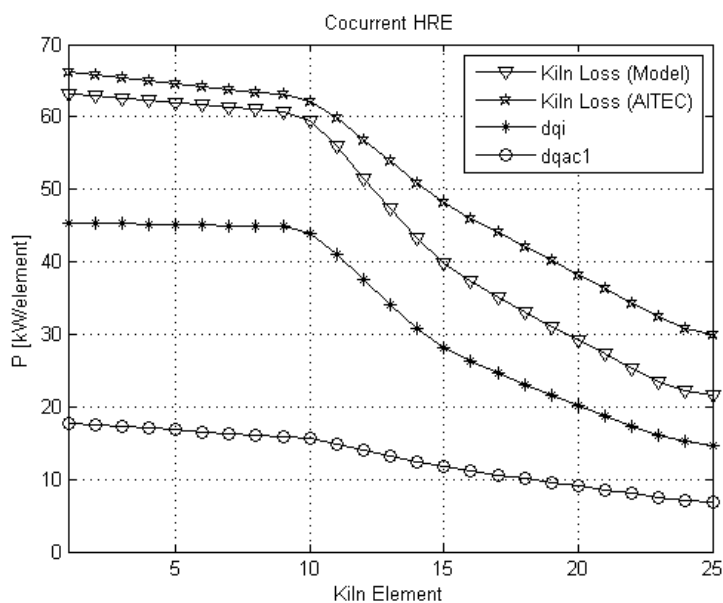


Figure 10. Trend of heat exchanged by kiln. Legend: Kiln loss (model) = overall heat lost by kiln walls when the HRE is installed; Kiln loss (AITEC) = overall heat dissipated by kiln walls in open air without HRE; dq_i = radiant heat transferred by kiln walls to water stream; dq_{ac1} = heat exchanged by convective transfer between kiln wall and air stream.

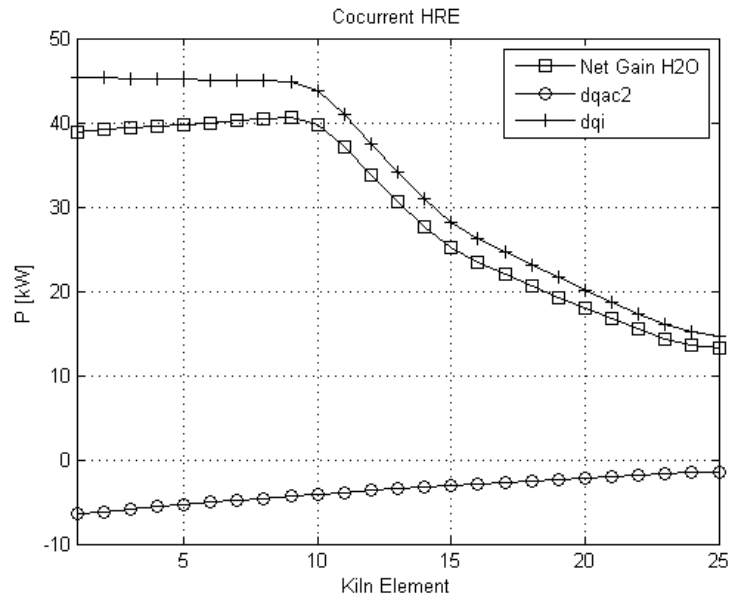


Figure 11. Trend of heat exchanged by water. Legend: Net gain H₂O = overall heat acquired by water stream; dq_j = radiant heat transferred by kiln walls to water stream; dq_{ac2} = heat exchanged by convective transfer between water and air stream.

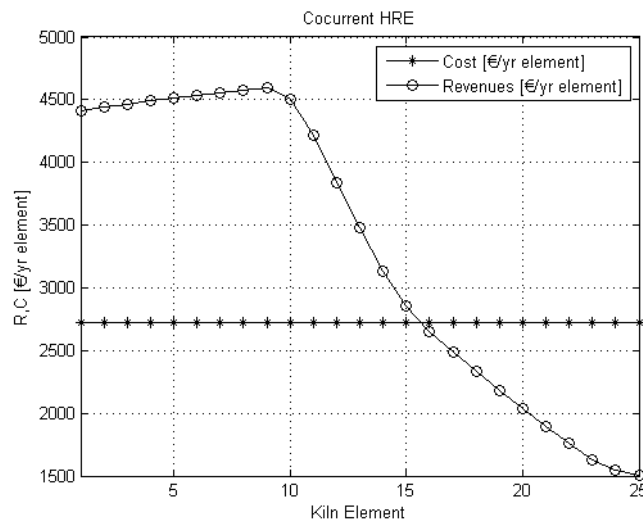


Figure 12 Annual revenues compared with equivalent annual cost on a section by section basis.

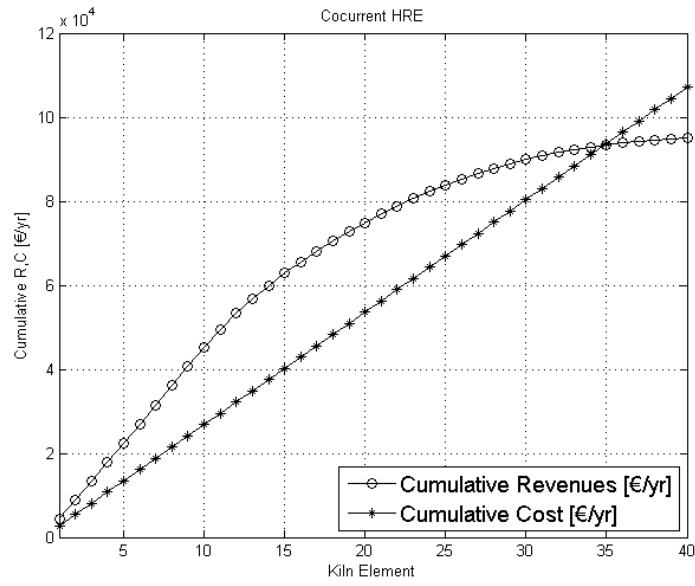


Figure 13. Cumulative annual revenues and capital investment vs HRE length.

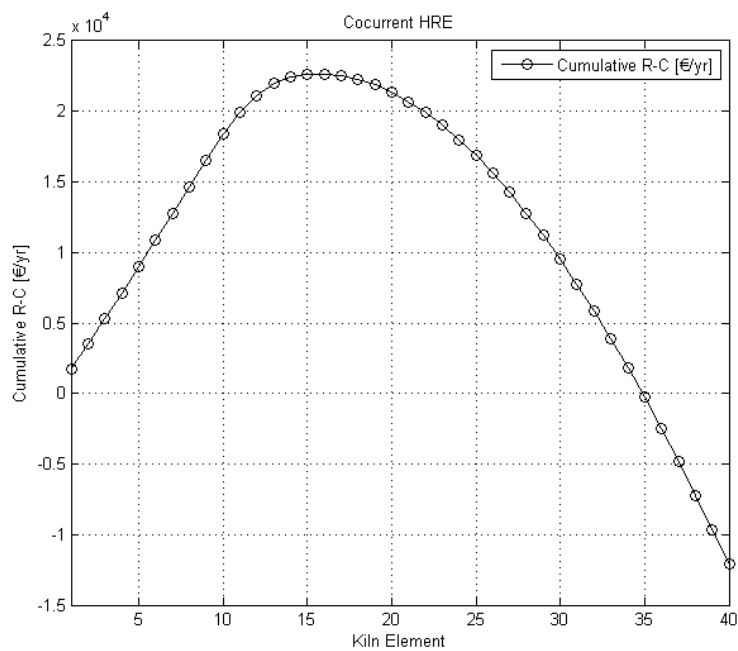


Figure 14. Cumulative net annual revenues vs HRE length.